

FIGURE 1: Task paradigm. (A) The task paradigm during the decoder training session. In the execute task, patients selected and executed 1 of 3 (or 5) movements after the sound cue. The cue consisted of 3 beeps 1 second apart that recurred every 5.5 seconds. The movements were performed with the arm contralateral to the implanted electrodes. In the attempt task, patients were instructed which of the 3 (or 5) movements to attempt. The 1-second electrocorticography (ECoG) signals used for the decoding analysis are shown below the time line: N = used for normalization and resting state; Pre = used as the first period by the Gaussian process regression (GPR) decoder; M = used as the move state; Post = as the last period by the GPR decoder. (B) Controlling the prosthetic hand with 2 decoders. The GPR decoder estimated the accuracy of the time determined to be necessary for the support vector machine (SVM) decoder to classify the ECoG signals. The prosthetic hand was controlled incrementally according to the decoding results.

classification accuracy of the SVM decoder. When the estimated classification accuracy exceeded a certain threshold value (see Fig 1B), the SVM decoder classified the ECoG signals to infer the intended movement (Supplementary Fig 3).

The GPR decoder was trained using a Gaussian process regression (GPR),²² which is one kind of Bayesian approach.²³ We used GPR because it could be applied to the nonlinear data with a simple model. The GPR decoder was trained with the classification accuracies and the 3 frequency band powers of 3 time domains (Pre, M, and Post in Fig 1A; see Supplementary Methods). The classification accuracies were evaluated by the mutual information, which quantified the confusion matrix resulting from the SVM decoder. The mutual information was normalized by using the values of the 3 time domains. The trained GPR decoder estimated the classification accuracy with 3 frequency band powers at a given time in a free-run session. The GPR and SVM decoders were trained for hand and elbow movements separately.

The commands to the prosthetic arm were updated by the host computer system every 200 milliseconds. When the SVM decoder inferred a movement type, the posture of the prosthetic arm was partially altered to match the posture of the inferred movement (see Supplementary Methods). Completing a movement required 2 or 3 consecutive matched decodings.

This incremental control of the prosthetic hand permitted the desired posture even when the classification performance of the SVM decoder was not perfect; the classification errors of the

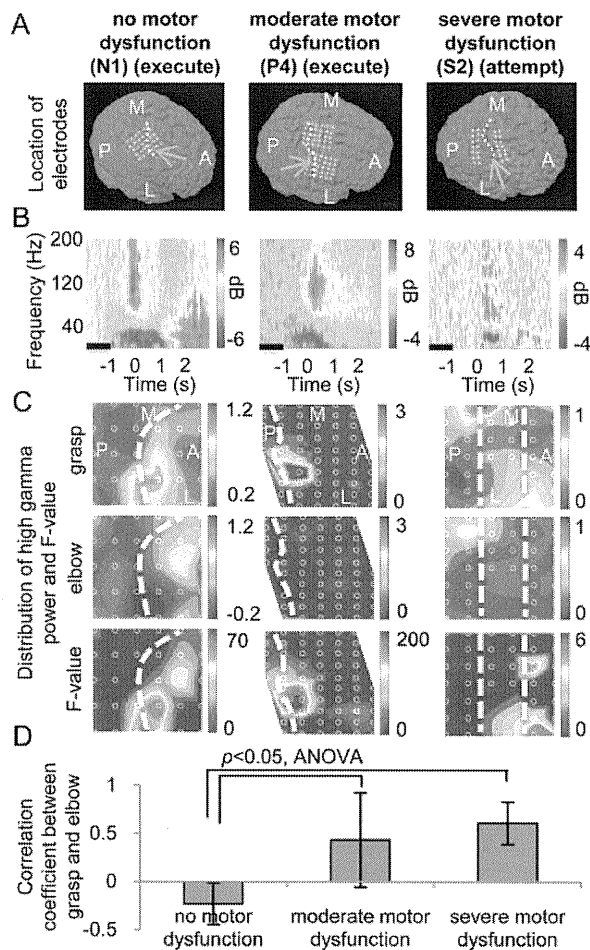


FIGURE 2: Representative results of time-frequency analysis. (A) Locations of implanted electrodes for patients N1, P4, and S2 are indicated by the green (implanted on the brain surface) and red (implanted within the central sulcus) filled circles on the 3-dimensional brain renderings of magnetic resonance imaging volumes. The dashed white line indicates the location of the central sulcus. Only the electrodes used for the analysis are shown. (B) Power spectra of the electrocorticographic signals recorded during grasping (execute) or attempt to grasp from the electrodes on the primary motor cortex indicated by the orange arrows in A. The black horizontal bars show the 1,000-millisecond period used for normalization. Time 0 corresponds to the onset cue. (C) The high gamma power is color coded to the location of the electrodes for grasping and elbow flexion. The direction indicators correspond to A = anterior, P = posterior, M = medial, and L = lateral on the brain. The white dashed lines and the white circles indicate the locations of the central sulcus and the electrodes, respectively. For the patient S2, the electrodes between the 2 white lines were located within the central sulcus (intrasulcal electrodes; see Supplementary Methods). The lowest figure of each patient shows the distribution of the F value with statistical significance ($p < 0.05$). (D) The correlation coefficient of the high gamma powers between hand grasping and elbow flexion for each patient's group. ANOVA = analysis of variance.

decoder caused only a tremor of the prosthetic arm as it moved to the desired posture.

Offline Analyses

The ECoG signals of grasping and elbow flexion were compared among patients. A Hilbert transformation (EEGLAB v5.03) was used to obtain the temporal power spectral density of each frequency band (see Supplementary Methods). The temporal powers were normalized by powers of the initial 1-second period (−2 to −1 seconds) of each trial.

The variability of the high gamma power of 0 to 1 second was statistically evaluated among 2 types of movements by the F value of one-way analysis of variance (ANOVA) for each electrode. The statistical similarity of the high gamma power maps was evaluated by determining the correlation coefficient of the mean power maps of 2 movements. The classification accuracies for inferring 2 movements using the SVM decoder with the high gamma powers were compared among patients.

Results

Time-Frequency Analysis

The power spectrum of the ECoG signals showed some characteristic modulations among patients. Figure 2B illustrates examples of the power spectrum time-locked to the external cues while grasping or attempting to grasp. An increase in the high gamma power and decreases in the alpha and beta powers were consistently observed for all patients with different levels of motor dysfunctions. The spatial distributions of the high gamma power during movement (0–1 second) were obviously different for each movement (see Fig 2C), and the ANOVA F value revealed that high gamma powers were significantly modulated between the movements. Notably, the powers around the central sulcus showed significant differences ($p < 0.05$). The characteristic modulations of the high gamma power were consistently observed among all patients, although the F values pertaining to variability were lower in patients with severe dysfunctions than in other patients. Moreover, the correlation coefficient of the spatial distribution of the high gamma power between the movements was significantly high for the patients with motor dysfunctions (see Fig 2D).

Decoding Analysis

The accuracy of classifying (ie, decoding) the movements was compared among the frequency band powers at each time. Figure 3 shows the color-coded percentage of correct movement classifications averaged over each patient group. Regardless of the level of motor dysfunctions, the 2 movement types were best inferred by using the high gamma power around the movement onset.

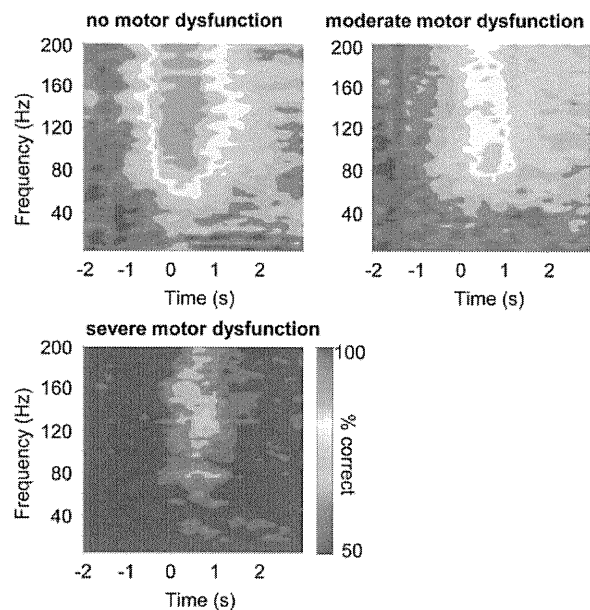


FIGURE 3: Averaged classification accuracy with each frequency band power. Classification accuracies with each frequency band power were averaged for the patients of each group and color coded at the center of each frequency band and time domain. Time 0 corresponds to the sound cue for the movements.

The movement classifications were carried out for all patients with a high gamma power for 0 to 1 seconds. The classification accuracy of patients S1 to S3 was significantly inferior to that of patients N1 to N5 (ANOVA, $p < 0.05$; see Table 2). However, these accuracies were still above levels that would occur by chance (50%). This relationship was also observed in the classification of 3 types of movements (Supplementary Table). On the other hand, the accuracies to classify the resting state (−2 to −1 seconds) and the movement state (0 to 1 seconds) were not significantly different among the 3 patient groups (see Table 2).

Decoding in Free-Run and Real-Time Control of a Prosthetic Hand

The classification accuracy of 3 hand movements with the SVM decoder varied with time in the decoder training session (Fig 4B). It was highest immediately after the onset cues (eg, when the hand EMG response started to increase; see Fig 4A). The trained GPR decoder accurately inferred the timing of the peak and zero value of the normalized mutual information only using the 3 frequency bands at each time (see Fig 4C).

Using the trained decoders, the ECoG signals were decoded in real time while the patient, without further training, voluntarily (ie, without cue) performed the 3 to 5 types of movements (free-run period, see Fig 4D). The estimated mutual information peaked when the standard

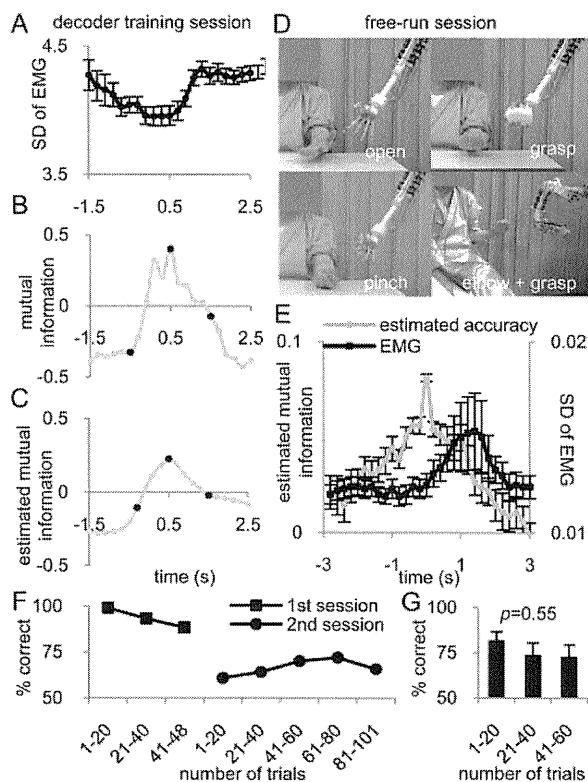


FIGURE 4: Prosthetic control with the electrocorticography (ECoG) signals. (A) The standard deviations (SDs) of the electromyographic (EMG) responses averaged over 1-second periods are shown at each time centered on the onset cue (0). (B) For patient P4, the mutual information for the performed movements and the inferred movements was normalized at each time. The values of the mutual information at 3 time domains (black circle) trained the Gaussian process regression (GPR) decoder. (C) The mutual information estimated by the trained GPR decoder at each time. (D) Representative photographs of the prosthetic arm controlled in real time by the ECoG signals of patient P4. (E) The estimated mutual information and standard deviation of the EMG responses were averaged for the 6 seconds time-locked to the peak values of the estimated mutual information that exceeded a value of 0.07. (F) The percentage correct of each 20 trials over the course of the entire free-run session of P4 (squares = first session; circles = second session). (G) The percentage correct of each 20 trials were not significantly different among all sessions of 4 patients (analysis of variance, $p = 0.55$).

deviation of the EMG response started to increase, indicating that the GPR decoder successfully decoded the movement onset in the free-run session (see Fig 4E).

The prosthetic arm was controlled in real time according to the decoding results of the SVM and GPR decoders, mimicking the hand movements of patients. The prosthetic hand completed the same movement of patient P4 in 42 of 48 attempts (87.5%; Supplementary Video 1). Each hand movement required an average of 2.2 incremental movements of 4.2 seconds each. By voluntarily moving his own hand, patient P4 was able to

catch and hold an object for seconds and intentionally release the object from the prosthetic hand (Supplementary Video 2). Moreover 4 days after the first experiments (second free run), the patient was still able to perform the same free-run task (Table 3, see Fig 4F, Supplementary Video 3), using the decoder trained in those initial experiments. The 3 other participating patients (N1, N3, N4) were also able to voluntarily control the prosthetic arm (see Table 3). Notably, the classification accuracy of the SVM decoder was not significantly different between the training session and the free-run session (ANOVA, $p = 0.06$) and over the course of the each free-run session (ANOVA, $p = 0.55$; see Fig 4F, G). Finally, the elbow of the prosthetic arm was simultaneously controlled by the other GPR decoder for the elbow (Supplementary Video 4). The success rate for complete elbow movements of the prosthetic arm was significantly lower than that of the training (ANOVA, $p < 0.05$).

Patient N1 described her impression of control as thinking at first that the prosthetic arm moved in mimicry of her movements, rather than that she was controlling the prosthesis. But at the end of the experiment, she realized she was able to control the prosthesis well. However, no patient controlling the prosthesis stopped moving their own limb.

Discussion

We have shown that ECoG signals recorded from patients with chronic motor dysfunctions still represented motor information via high gamma power to a degree that they could be decoded successfully enough to control a prosthetic hand. However, the modulation of the representation for different movements may have deteriorated depending on the degree of impairment. Our quantitative evaluation of motor representations in the reorganized cortex elucidated pathological states of patients with motor dysfunctions and demonstrated the applicability of these representations for an ECoG-based BCI to improve patients' quality of life.

Preserved Features following Cortical Reorganization

The spatiotemporal features of the ECoG signals during movements or attempts at movements were qualitatively preserved in the sensorimotor cortex of impaired patients. During movements, high gamma power was consistently increased around the central sulcus, even for severely impaired patients. This is consistent with previous functional magnetic resonance imaging (fMRI) studies showing that activation of the motor cortex is

TABLE 3: Summary of the Real-Time Control of the Prosthetic Hand

Patient No. and Session	Hand Movements (grasp, pinch, open)				Elbow Movements (flexion, extension)				
	% Correct of Training	% Correct to Complete (correct/trial)	% Correct of SVM Decoder in Free Run	Time/Count to Complete (s/count)	% Correct of Training	% Correct to Complete (correct/trial)	% Correct of SVM Decoder in Free Run	Time/Count to Complete (s/count)	
N1	1st	79.2	71.2 (37/52)	76.1	1.8/3.3	64.3	—	—	—
	2nd		51.2 (22/43)	67.0	1.5/3.3				
N3	1st	70.0	85.7 (30/35)	80.7	1.6/3.3	77.5	14.3 (1/7)	87.5	13.6/3
	2nd		47.2 (17/36)	81.0	1.3/2.7				
N4	1st	60.8	64.7 (11/17)	70.3	1.3/3.7	74.0	33.3 (1/3)	60.0	3.3/2
	2nd		—	—	—				
P4	1st	80.8	87.5 (42/48)	68.8	2.2/4.2	70.0	54.2 (26/48)	90.1	2.3/3.7
	2nd		62.3 (63/101)	62.3	2.0/4.1				
Mean ± SD		72.7 ± 9.2	77.3 ± 11.1	74.0 ± 5.5	1.7 ± 0.4/ 3.6 ± 0.4	71.5 ± 5.7	33.9 ± 20.0 (<i>p</i> < 0.05, ANOVA)	79.2 ± 16.7	6.4 ± .6.3/ 2.9 ± 0.9
			53.6 ± 7.8	70.1 ± 9.7	1.6 ± 0.4/ 3.6 ± 0.7				

ANOVA = analysis of variance; SVM = support vector machine.

preserved even in paralyzed patients,^{24–26} because the high gamma activity is correlated with the fMRI blood oxygen level-dependent signal.²⁷

The decoding analysis showed that modulation of the high gamma power provided the most information about the movement types. This result was consistent with previous studies that showed human movements could be inferred by using ECoGs.^{3,4,28,29} It was suggested that the basic features of cortical processing with high gamma powers are preserved following cortical reorganization resulting from motor dysfunctions.

Deteriorated Motor Representation Accompanying Phantom Limb Pain

The decreased decoding accuracy in patients with motor dysfunctions indicated that the high gamma powers were not prominently modulated among the different types of movements, suggesting that modulation of the high gamma power (ie, motor representation) had significantly deteriorated following cortical reorganization. Conversely, the increased correlation of the high gamma powers between different movements suggested that the representations of the movements became similar to each other in the impaired patients. Notably, this similarity was not due to a weakened representation; an increase in the high gamma power during movement was accurately decoded even in the patients with severe dysfunctions. Our results suggested that the modulation of the high gamma powers had deteriorated in the impaired patients with increased similarity of the power maps among movements. This result was consistent with previous reports showing that cortical representations of nonaffected body parts shifted to overlap representations of affected body parts in phantom limb pain patients.^{11,16,30} It was suggested that the decreased decoding accuracy of movement types might be due to overlaps in the spatial distributions of the high gamma powers for each movement.

Our data also suggested that the deteriorated modulation of motor representations in patients S1 to S3 was related to patients' ability to imagine movements. Classification accuracy of these patients was highest for the patient who could most easily imagine the movements and lowest for the patients who could hardly imagine movements. This relation was also observed in the distribution of the *F* values of the high gamma powers (Supplementary Fig 4). For some patients who lost the ability to imagine intentionally moving their phantom limbs, the motor representation, or high gamma powers, may no longer be modulated well enough to be decoded. We suggest that cortical reorganization did not alter the characteristic features of the ECoG signals, but rather affected modulation of the representation, related to the ability to imagine the movements.

Prosthetic Hand Control Applied to a Diverse Patient Population

Successful control of the prosthetic arm was demonstrated with the SVM and GPR decoders, which accurately inferred various movement types from the ECoG signals of patients with motor dysfunctions. This suggests the feasibility of restoring purposeful movement based on a BCI. Although the cortical control of some prostheses has already been demonstrated with other invasive signals,^{31,32} our success with the ECoG signals may be beneficial for clinical applications because an ECoG-based BCI has advantages in signal stability and durability that are absolutely necessary for clinical application.² As we demonstrated, the prosthetic hand could be controlled for several days with a single decoder trained once at the first session. This reveals the robustness of our decoding method and the stability of the ECoG signals. Moreover, our method was demonstrated with an elderly patient who was able to successfully and naturally control the prosthetic arm without any prior training. A requisite for a clinically useful BCI system is that it be developed to be stably and easily used by a diverse population of patients in their daily lives.

Acknowledgments

This work was supported in part by the Strategic Research Program for Brain Sciences of Ministry of Education, Culture, Sports, Science and Technology-Japan (MEXT); KAKENHI (22700435); Nissan Science Foundation; Ministry of Health, Labor, and Welfare (18261201); and Strategic Information and Communications R&D promotion Programme (SCOPE), SOUMU.

Potential Conflicts of Interest

Nothing to report.

References

1. Leuthardt EC, Schalk G, Moran D, et al. The emerging world of motor neuroprosthetics: a neurosurgical perspective. *Neurosurgery* 2006;59:1–14.
2. Chao ZC, Nagasaka Y, Fujii N. Long-term asynchronous decoding of arm motion using electrocorticographic signals in monkeys. *Front Neuroeng* 2010;3:3.
3. Pistohl T, Ball T, Schulze-Bonhage A, et al. Prediction of arm movement trajectories from ECoG-recordings in humans. *J Neurosci Methods* 2008;167:105–114.
4. Schalk G, Miller KJ, Anderson NR, et al. Two-dimensional movement control using electrocorticographic signals in humans. *J Neural Eng* 2008;5:75–84.
5. Schalk G, Kubanek J, Miller KJ, et al. Two-dimensional movement trajectories using electrocorticographic signals in humans. *J Neural Eng* 2007;4:264–275.

6. Miller KJ, Zanos S, Fetz EE, et al. Decoupling the cortical power spectrum reveals real-time representation of individual finger movements in humans. *J Neurosci* 2009;29:3132–3137.
7. Bruehlmeier M, Dietz V, Leenders KL, et al. How does the human brain deal with a spinal cord injury? *Eur J Neurosci* 1998;10:3918–3922.
8. Green JB, Sora E, Bialy Y, et al. Cortical motor reorganization after paraplegia: an EEG study. *Neurology* 1999;53:736–743.
9. Mikulis DJ, Jurkiewicz MT, McIlroy WE, et al. Adaptation in the motor cortex following cervical spinal cord injury. *Neurology* 2002;58:794–801.
10. Ramachandran VS, Rogers-Ramachandran D, Stewart M. Perceptual correlates of massive cortical reorganization. *Science* 1992;258:1159–1160.
11. Flor H. Phantom-limb pain: characteristics, causes, and treatment. *Lancet Neurol* 2002;1:182–189.
12. Roricht S, Meyer BU, Niehaus L, et al. Long-term reorganization of motor cortex outputs after arm amputation. *Neurology* 1999;53:106–111.
13. Green JB. Brain reorganization after stroke. *Top Stroke Rehabil* 2003;10:1–20.
14. Nudo RJ, Wise BM, SiFuentes F, et al. Neural substrates for the effects of rehabilitative training on motor recovery after ischemic infarct. *Science* 1996;272:1791–1794.
15. Gerloff C, Bushara K, Sailer A, et al. Multimodal imaging of brain reorganization in motor areas of the contralesional hemisphere of well recovered patients after capsular stroke. *Brain* 2006;129:791–808.
16. Flor H, Elbert T, Knecht S, et al. Phantom-limb pain as a perceptual correlate of cortical reorganization following arm amputation. *Nature* 1995;375:482–484.
17. Hosomi K, Saitoh Y, Kishima H, et al. Electrical stimulation of primary motor cortex within the central sulcus for intractable neuropathic pain. *Clin Neurophysiol* 2008;119:993–1001.
18. Yanagisawa T, Hirata M, Saitoh Y, et al. Neural decoding using gyral and intrasulcal electrocorticograms. *Neuroimage* 2009;45:1099–1106.
19. Yanagisawa T, Hirata M, Saitoh Y, et al. Real-time control of a prosthetic hand using human electrocorticography signals. *J Neurosurg* 2011;114:1715–1722.
20. Kamitani Y, Tong F. Decoding the visual and subjective contents of the human brain. *Nat Neurosci* 2005;8:679–685.
21. Kamitani Y. Brain decoder toolbox. 2010. Available at: <http://www.cns.atr.jp/dni/en/downloads/brain-decoder-toolbox>. Assessed on 12 May 2010.
22. Ebden M. Gaussian processes for regression: a quick introduction. Available at: <http://www.robots.ox.ac.uk/~mebden/reports/GPTutorial.pdf>. Assessed on 15 December 2010.
23. Rasmussen C, Williams C. Gaussian processes for machine learning. Cambridge, MA: MIT Press, 2006.
24. Shoham S, Haigren E, Maynard EM, et al. Motor-cortical activity in tetraplegics. *Nature* 2001;413:793.
25. Corbetta M, Burton H, Sinclair RJ, et al. Functional reorganization and stability of somatosensory-motor cortical topography in a tetraplegic subject with late recovery. *Proc Natl Acad Sci USA* 2002;99:17066–17071.
26. Cramer SC, Lastra L, Lacourse MG, et al. Brain motor system function after chronic, complete spinal cord injury. *Brain* 2005;128:2941–2950.
27. Logothetis NK, Pauls J, Augath M, et al. Neurophysiological investigation of the basis of the fMRI signal. *Nature* 2001;412:150–157.
28. Kubanek J, Miller KJ, Ojemann JG, et al. Decoding flexion of individual fingers using electrocorticographic signals in humans. *J Neural Eng* 2009;6:1–14.
29. Crone NE, Sinai A, Korzeniewska A. High-frequency gamma oscillations and human brain mapping with electrocorticography. *Prog Brain Res* 2006;159:275–295.
30. Karl A, Birbaumer N, Lutzengerger W, et al. Reorganization of motor and somatosensory cortex in upper extremity amputees with phantom limb pain. *J Neurosci* 2001;21:3609–3618.
31. Velliste M, Perel S, Spalding MC, et al. Cortical control of a prosthetic arm for self-feeding. *Nature* 2008;453:1098–1101.
32. Hochberg LR, Serruya MD, Friehs GM, et al. Neuronal ensemble control of prosthetic devices by a human with tetraplegia. *Nature* 2006;442:164–171.

A Prospective, Open-Label, Multicenter Study to Assess the Efficacy of Spinal Cord Stimulation and Identify Patients Who Would Benefit

Kazuhide Moriyama, MD, PhD*, Kazushige Murakawa, MD, PhD*, Takeshi Uno, MD, PhD[†], Kiyoshige Oseto, MD, PhD[‡], Minoru Kawanishi, MD, PhD[§], Yoichi Saito, MD, PhD[¶], Takaomi Taira, MD, PhD^{**}, Masanori Yamauchi, MD, PhD^{††}

Objective: To identify patients likely to benefit from spinal cord stimulation (SCS).

Materials and Methods: This multicenter, prospective, open-label study included medical centers experienced in SCS therapy, carried out in 13 physicians in seven centers. We recruited 55 patients with complex regional pain syndrome, failed back surgery syndrome, or peripheral vascular disease. Neurostimulators were implanted in 34 patients found to respond to SCS in a preliminary test, who were then followed for six months. Thirty-four patients scored their pain on a visual analog scale (VAS) and completed the EuroQol-5D questionnaire before and after test stimulation and after one and six months.

Results: During test stimulation, the mean VAS and quality of life (QOL) scores improved from 74.0 to 23.4 and from 0.430 to 0.664, respectively, in the 34 patients. At six months, the mean VAS score was 29.7 in 29 patients and the mean QOL score was 0.661 in 31 patients.

Conclusion: SCS may improve pain management and QOL.

Keywords: EQ-5D, neuropathic pain, pain relief, quality of life, spinal cord stimulation

Conflict of Interest: The authors reported no conflict of interest.

INTRODUCTION

In Japan, spinal cord stimulation (SCS) has been used since 1982 for the treatment of chronic pain symptoms, such as neuropathic pain, not responsive to other therapies. We conducted this study with the aims of relieving pain and improving quality of life (QOL) for patients (1). Of the approximately 1.1 million patients with neuropathic pain in Japan (2,3), only an estimated 4000 are treated by SCS. This is because nerve block is generally the first choice of therapy, with SCS being reserved for patients unresponsive to nerve block (1,4,5). However, when other therapies fail to relieve pain, SCS might be less effective once that pain has become chronic (6).

We designed this multicenter, prospective, open-label study to characterize patients most likely to benefit from SCS and to evaluate the efficacy of this treatment modality in *chronic* patients. Our goal is to identify features possibly facilitating wider and more efficient use of SCS.

METHODS

We recruited patients with failed back surgery syndrome (FBSS) (7,8), complex regional pain syndrome (CRPS) (9,10), or peripheral vascular disease (PVD) (11). Study registration started on August 3, 2006, and ended on February 15, 2008. Follow-up was completed on September 4, 2008.

Study Design

The study had a multicenter, prospective, open-label design. The investigation involved a preimplantation evaluation, a screening trial period, and follow-up evaluations conducted at one and six months (details given below). Clinical end points included changes in scores on a visual analog scale (VAS) and the EuroQol-5D (EQ-5D) questionnaire from screening trial stimulation until final follow-up.

Address correspondence to: Kazuhide Moriyama, MD, PhD, Department of Pain Medicine, Hyogo College of Medicine, 1-1 Mukogawa-cho, Nishinomiya, Hyogo 663-8501, Japan. Email: pain-med@hyo-med.ac.jp

* Department of Pain Medicine, Hyogo College of Medicine, Hyogo, Japan;

[†] Department of Pain Clinic, Junwakai Memorial Hospital, Miyazaki, Japan;

[‡] Department of Pain Clinic, Kanto Medical Center NTT EC, Tokyo, Japan;

[§] Department of Anesthesiology, Banbuntane Houtokukai Hospital, Aichi, Japan;

[¶] Department of Neurosurgery, Osaka University, Osaka, Japan;

** Department of Neurosurgery, Tokyo Women's Medical University, Tokyo, Japan; and

^{††} Department of Anesthesiology, Sapporo Medical University, Hokkaido, Japan

For more information on author guidelines, an explanation of our peer review process, and conflict of interest informed consent policies, please go to <http://www.wiley.com/bw/submit.asp?ref=1094-7159&site=1>

Source of funding: This study was supported by a grant from Medtronic Japan Co., Ltd.

Test Stimulation and SCS Device Implantation

Patients who met the selection criteria (Table 1) and provided written informed consent were recruited for the study. These patients underwent a screening trial of the neurostimulator (Pisces Quad lead model 3487A, 3887, Synergy V, model 7427V; Medtronic Inc., Minneapolis, MN, USA). Patients were allowed to choose either the puncture method trial or surgery at the time of providing informed consent. Before and after the test stimulation in this trial, patients evaluated their pain intensity on a 10-cm VAS in which the point farthest to the left represented no pain (score: 0) and that farthest to the right represented the worst possible pain (score: 100). A screening trial was considered to be successful when the VAS score decreased by at least 50% vs. the score prior to stimulation. If the screening trial was not successful, the leads were removed, and the patient was withdrawn from the study. Patients with a successful screening trial and who wanted to use the Synergy V were enrolled in the study, and the stimulator was permanently implanted. All data on case report forms were recorded by patients themselves.

Evaluation During Follow-Up

All patients were asked to score their pain on the VAS and to complete the EQ-5D questionnaire (12) at the following time points: before trial stimulation, after trial stimulation, and at the one- and six-month follow-ups. We used the portion of the two-part EQ-5D that recorded self-reported health problems in five dimensions: mobility, self-care, usual activities, pain or discomfort, and anxiety or depression. Each dimension was subdivided into three categories: no, moderate, and extreme problems. The utility value was calculated by applying an appropriate weighting system obtained from the EuroQol Group.

Statistical Analysis

Changes in variables were tested using a paired *t*-test, and factors influencing changes were evaluated using a mixed effect model with the patient as a random effect. *p*-values < 0.05 were considered statistically significant.

Table 1. Selection Criteria.

Inclusion

1. Patients with chronic pain of unknown origin meeting at least one of the following criteria:
Pain continuing for at least one month after resolution of acute tissue injury
Pain continuing for at least three months or recurrent pain
Continuous or progressive pain related to tissue injury
2. Eighteen years of age or older
3. Resistant to pharmacological or physical therapy
4. One of the following disease types:
Failed back surgery syndrome
Complex regional pain syndrome
Peripheral vascular disease

Exclusion

1. Remaining active life predicted to be less than one year
2. Mental illness
3. Pregnant or likely to become pregnant
4. Pacemaker, implantable cardioverter-defibrillator, or diathermy
5. Likely to undergo magnetic resonance imaging

We defined a response as a 50% or more reduction in pain VAS scores during the screening trial. To select predictors of response, logistic regression was applied with the stepwise selection method and a 0.01 significance level.

RESULTS

Table 2 summarizes the characteristics of the 55 patients who underwent test stimulation. There were 24 women and 31 men, 25–80 years of age. Five, 22, and 28 patients had PVD, CRPS, and FBSS, respectively. The mean (\pm standard deviation) values for pain duration, number of pain sites, and cover rate (the number of patients reporting pain at a given site) were 67.8 months (\pm 73.1), 16.4 (\pm 12.4), and 81.8% (\pm 21.1), respectively. SCS devices were permanently implanted in 34 patients, 18 women and 16 men ranging in age from 25 to 80 years (CRPS, *N* = 14; FBSS, *N* = 17; and PVD, *N* = 3). These 34 patients were considered to be responders to SCS because they had shown a 50% pain reduction on the VAS, with the trial stimulation. A dual lead was used in 26 patients and a single lead in eight. Single leads were used in some cases because stimulation adequate to mask pain could be achieved.

Of these 34 patients, 31 were observed at the one-month and 29 at the six-month follow-up. The remaining patients have yet to be followed up.

VAS and EQ-5D

The results of the VAS and EQ-5D are shown in Table 3. At all follow-up points, the VAS and EQ-5D scores for pain intensity were

Table 2. Patient Characteristics.

	Test stimulation <i>N</i> = 55	Permanent implantation <i>N</i> = 34
Age (years), mean (SD)	51.9 (15.9)	53.5 (16.9)
Gender, no. (%)		
Female	24 (43.6)	18 (52.9)
Male	31 (56.4)	16 (47.1)
Pain duration (m), mean (SD)	67.8 (73.1)	67.8 (73.1)
Visual analog scale (mm), mean (SD)	74.3 (21.0)	74.0 (21.4)
EuroQol-5D utility value, mean (SD)	0.430 (0.180)	0.430 (0.169)
Disease, no. (%)		
CRPS	22 (40.0)	14 (41.2)
FBSS	28 (50.9)	17 (50.0)
PVD	5 (9.1)	3 (8.8)
Part of nervous system affected, no. (%)		
Central	8 (15.1)	3 (9.1)
Peripheral	45 (84.9)	30 (90.9)
Pain type, no. (%)		
Nociceptive	2 (3.7)	1 (2.9)
Neuropathic	47 (87.0)	30 (88.2)
Mixed	5 (9.3)	3 (8.8)
Pain pattern, no. (%)		
Unilateral	25 (46.3)	14 (41.2)
Bilateral	27 (50.0)	18 (52.9)
Mixed	2 (3.7)	2 (5.9)
Number of pain sites, mean (SD) (<i>N</i> = 54)	16.4 (12.4)	16.9 (12.7)
Cover rate* (%), mean (SD) (<i>N</i> = 54)	81.8 (21.1)	87.8 (15.1)
Number of nerve blocks, mean (SD)	1.7 (2.3)	1.7 (2.0)

*The number of patients reporting pain at a given site.
CRPS, complex regional pain syndrome; FBSS, failed back surgery syndrome; PVD, peripheral vascular disease; SD, standard deviation.

Table 3. Summary of VAS Scores and EQ-5D Utility Values.

	Test stimulation			After	One-month follow-up			Six-month follow-up				
	Before	Mean	SD		N	Mean	SD	N	Mean	SD		
VAS												
Total	34	74.0	21.4	34	23.4	13.0	31	29.4	17.6	29	29.7	25.8
CRPS	14	79.6	21.9	14	26.1	12.1	12	28.8	15.5	12	22.4	20.3
FBSS	17	68.9	22.2	17	22.7	13.6	17	32.5	18.3	15	39.5	27.2
PVD	3	76.0	6.9	3	14.7	12.9	2	7.0	9.9	2	0.0	0.0
Change in VAS score from before the test stimulation												
Total				34	-50.6*	19.2	31	-45.4*	23.7	29	-46.5*	30.8
CRPS				14	-53.6*	20.6	12	-54.6*	19.6	12	-60.9*	23.5
FBSS				17	-46.2*	18.0	17	-36.4*	23.6	15	-31.3*	30.3
PVD				3	-61.3*	18.0	2	-67.0	18.4	2	-74.0	8.5
VAS response				N	(%)		N	(%)		N	(%)	
Total				34	100.0		25	80.6		19	65.5	
CRPS				14	100.0		11	91.7		10	83.3	
FBSS				17	100.0		12	70.6		7	46.7	
PVD				3	100.0		2	100.0		2	100.0	
EQ-5D utility value												
Total	34	0.430	0.163	34	0.664	0.207	31	0.682	0.211	31	0.661	0.177
CRPS	14	0.425	0.178	14	0.640	0.239	12	0.607	0.201	12	0.602	0.170
FBSS	17	0.466	0.099	17	0.680	0.180	17	0.726	0.205	17	0.663	0.148
PVD	3	0.242	0.306	3	0.689	0.270	2	0.767	0.330	2	1.000	0.000
Change in EQ-5D utility value from before test stimulation												
Total				34	0.235*	0.225	31	0.266*	0.214	31	0.228*	0.181
CRPS				14	0.215*	0.277	12	0.217*	0.259	12	0.212*	0.221
FBSS				17	0.213*	0.151	17	0.260*	0.151	17	0.197*	0.104
PVD				3	0.446	0.290	2	0.613*	0.045	2	0.581	0.000

*Statistically significant change vs. before the test stimulation ($p < 0.05$).

CRPS, complex regional pain syndrome; EQ-5D, EuroQol-5D; FBSS, failed back surgery syndrome; PVD, peripheral vascular disease; SD, standard deviation; VAS, visual analog scale.

both decreased as compared with before the test stimulation. Most patients remained responsive to SCS, the exception being those with FBSS (Table 3, Fig. 1).

A mixed model analysis (Table 4) showed that patients with FBSS demonstrated a significantly smaller change in VAS scores than those with CRPS or PVD ($p = 0.02$); the difference was 23.1 mm. However, this pattern was not seen for the EQ-5D utility values. For both the VAS and the EQ-5D scores, the one- and six-month follow-up results were similar.

Relationship Between Response and Patient Characteristics

A logistic model with the response to test stimulation as a response variable was used to determine predictors of the response to SCS. Candidate predictors were age (year), gender, pain duration (months), VAS score (mm) before the test stimulation, the part of the nervous system affected, pain type, pain pattern, number of pain sites, and cover rate (%). These were subject to univariate analysis followed by stepwise selection. Cover rate, gender, and the part of the nervous system affected were selected as predictors. Table 5 shows the results of the prediction model for 53 patients (33 responders and 20 nonresponders). Patients who had paresthesia covering a substantial portion of the painful area, women, and those with disorders affecting the peripheral nervous system were more responsive to SCS than other study subjects. Using this model, the response was correctly predicted in 28 of the 33 responders with

VAS (mm)

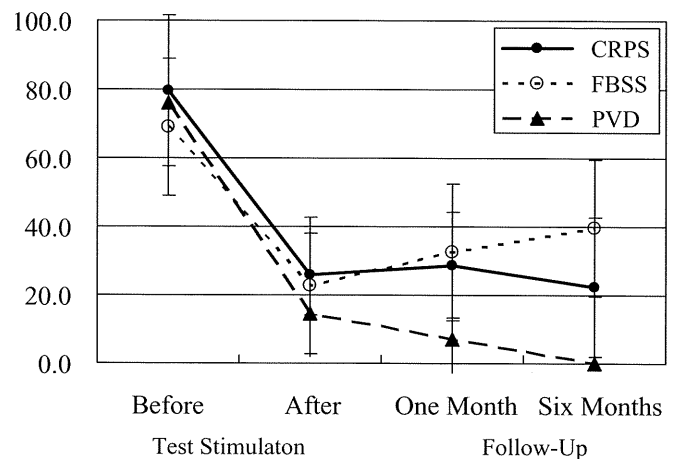


Figure 1. Change in VAS scores (mean, SD [mm]) for each disease. CRPS, complex regional pain syndrome; FBSS, failed back surgery syndrome; PVD, peripheral vascular disease; SD, standard deviation; VAS, visual analog scale.

a cutoff probability of 0.50; hence, sensitivity was 84.8% (28/34). Nonresponse was correctly predicted in 14 of the 20 nonresponders; thus, specificity was 70% (14/20). Accuracy was 79.2% (42/53) and the positive predictive value was 82.4% (28/34).

Table 4. Differences of Least-Squares Means in the Mixed Model.

Effect	Estimate	SE	df	t-value	Pr > t
Change in VAS score from before the test stimulation					
FBSS vs. CRPS or PVD	23.0681	9.393	28	2.46	0.0205
One month vs. six months	-1.1988	5.8956	28	-0.2	0.8403
Change in EQ-5D utility value from before the test stimulation					
FBSS vs. CRPS and PVD	0.01827	0.06326	28	0.29	0.7748
One month vs. six months	0.03777	0.03098	28	1.22	0.2330

Changes were treated as response variables. Values before the test stimulation, diagnosis (FBSS vs. CRPS or PVD), and follow-up period (one month vs. six months) were treated as explanatory variables.
 CRPS, complex regional pain syndrome; df, degree of freedom; EQ-5D, EuroQol-5D; FBSS, failed back surgery syndrome; PVD, peripheral vascular disease; SE, standard error of the mean; VAS, visual analog scale.

Table 5. Logistic Model for Prediction of Response ($N = 53$).

Analysis of maximum likelihood estimates						Odds ratio estimates		
Parameter	df	Estimate	SE	Wald chi-square	p-value	Point estimate	95% Wald LCL	UCL
Intercept	1	-3.5533	1.3921	6.52	0.0107			
Cover rate (%)	1	0.0460	0.0166	7.71	0.0055	1.047	1.014	1.082
Female vs. male	1	0.7179	0.3583	4.01	0.0451	4.203	1.032	17.119
Central vs. peripheral	1	-0.7471	0.4411	2.87	0.0903	0.224	0.040	1.264

df, degree of freedom; SE, standard error of the mean; LCL, lower confidence limit; UCL, upper confidence limit.

DISCUSSION

Pharmacological and physical therapies are the methods of first choice for pain relief in Japan. If these therapies fail, SCS may be suggested. Although nearly 4000 patients have undergone SCS in Japan, our experiences with SCS are inadequate to determine which patients are most likely to benefit from this treatment.

In the present study, 34 (61.8%) of the 55 patients initially recruited responded to test stimulation. However, because the test stimulation process is invasive, we sought to improve the response rate. The logistic regression analysis results (Table 5) suggest Synergy V implantation to be more appropriate for patients who have paresthesia covering a substantial portion of the painful area, are female, or have pain involving the peripheral nervous system. Using this model, the success rate of test stimulation may be improved to 82.4% (the positive predictive value of this model). However, application may be limited because the prediction model was constructed from a small sample and with limited patient information. While the prediction model appears to be reasonable, more complete patient information might allow a model with greater precision to be developed. Such a model would facilitate determining which patients will respond to SCS.

The mechanism by which SCS (5) ameliorates pain appears to involve paresthesia covering an extensive portion of the pain-affected area. This is consistent with the findings of the model employed in this study. The Synergy V has dual leads and therefore produces greater pain coverage than previously used SCS devices. This suggests that the Synergy V provides superior pain relief.

The principle of SCS is direct stimulation of the spinal cord. This implies that SCS should be more effective in the treatment of peripheral than central nervous system pain, and this was borne out by the model. We have no explanation at present as to why the female gender was a predictor of response, and there may be other as yet unknown covariates that confound with sex.

In this study, the pain VAS score was reduced from an average of 74.0 to 13.0 mm by test stimulation in responders, and most patients maintained these effects for six months. However, SCS had less effect on the pain of FBSS patients than on that of CRPS and PVD patients, with a difference of approximately 20 mm on VAS. This may be because SCS mainly affects neuropathic pain, and FBSS is characterized by a mixture of nociceptive and neuropathic forms of pain. Moreover, pain is limited to the limbs in CRPS, while affecting both limbs and the trunk in FBSS. Based on anatomic and physiologic factors influencing pain sensitivity, limb pain appears to be more sensitive to SCS treatment than trunk pain. When used for patients with FBSS, CRPS, or PVD, SCS is expected to be effective in those in whom epidural block exerts reliable effects even temporarily. However, SCS is often ineffective in cases with pain closely related to nociceptive elements (i.e., pain moderately or more reactive to opioids) because stimulation paresthesia is unlikely to show overlap. These findings appear to be consistent with the observations that pain involving the trunk often responds well to opioids in patients with FBSS and that lower back pain of a neuropathic nature, not accompanied by any other type of pain, is relatively rare in patients with FBSS (as in patients with other degenerative spinal disease). In patients with FBSS or CRPS, the efficacy of SCS is unreliable when affected by psychologic factors. Thus, whether or not individual patients are indicated for SCS must be determined carefully.

This implies that an opioid test (13) may be needed to determine whether the opioid nociceptive factor is present in FBSS patients before attempting SCS treatment. However, although VAS changes differed between FBSS and other diseases, QOL changes did not (Fig. 2). Therefore, we may need to consider the effect of muscle pain due to increased activities of daily living. Furthermore, when using SCS, it may be important to ascertain QOL status in order to control this muscle pain.

In patients with PVD, the timing of SCS is important. If SCS is applied to PVD cases in whom evaluation of intermittent limping is

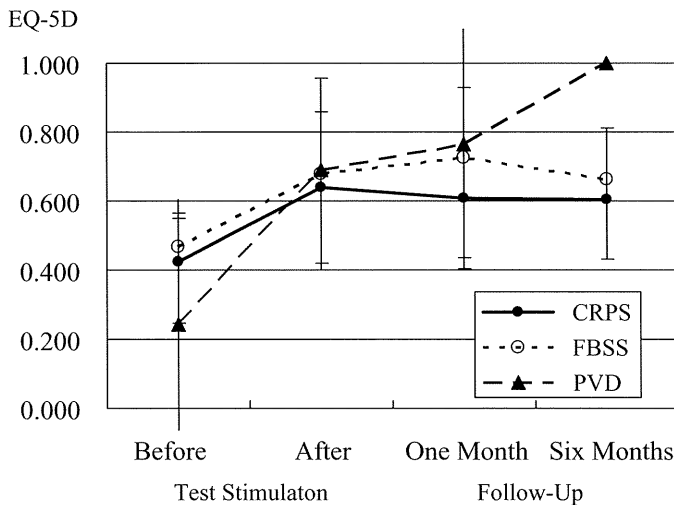


Figure 2. Change in EQ-5D utility values (mean, SD) for each disease. CRPS, complex regional pain syndrome; EQ-5D, EuroQol-5D; FBSS, failed back surgery syndrome; PVD, peripheral vascular disease; SD, standard deviation.

possible (i.e., PVD cases capable of walking to some extent), SCS can be expected to increase muscular oxygen demand and stimulate the growth of collaterals (14).

CONCLUSIONS

In conclusion, patients with paresthesia covering an extensive portion of the painful area and with peripheral nervous system involvement may be the most appropriate candidates for SCS. We intend to use SCS for the treatment of long-standing neuropathic pain symptoms not relieved by other therapies in order not only to relieve this form of pain at an early stage but also to improve the QOL of affected patients. Our hope is that this intervention will prevent neuropathic pain from progressing to a severe chronic stage (15–17).

Acknowledgements

The authors thank the following colleagues: Akiyoshi Namiki, Fujio Yanamoto, Yoichiro Abe, Mikito Kawamata, Shingo Tateyama, and Shinichi Goto.

Authorship Statements

All the doctors from the seven centers designed and conducted the study, including patient recruitment and data collection. We gathered an advisory board meeting three times. All authors approved the final manuscript.

How to Cite this Article:

Moriyama K., Murakawa K., Uno T., Oseto K., Kawanishi M., Saito Y., Taira T., Yamauchi M. 2011. A Prospective, Open-Label, Multicenter Study to Assess the Efficacy of Spinal Cord Stimulation and Identify Patients Who Would Benefit. *Neuromodulation* 2012; 15: 7–12

REFERENCES

1. Tsubokawa T. The use of the implantable stimulator, "ITREL3," for relief of chronic pain. *Pain Res* 1997;12:139–146. (In Japanese).
2. Anterio Inc. Product performance report. Medtronic Japan Co, Ltd. 2009.
3. Hattori S, Takeshima N, Kimura N, Yamamoto K, Mizutani A, Noguchi T. The clinical perspective on chronic pain management in Japan. *Pain Clinic* 2004;25:1541–1551.
4. Committee on the Guidelines for Pain Treatment, the Japan Society of Pain Clinicians. Analyses of questionnaires on the second revision of the guidelines for pain treatment published by the Japanese Society of Pain Clinicians. *Journal of Japan Society of Pain Clinicians* 2009;16:30–37.
5. Murakawa K, Moriyama K, Noma H, Yasuoka H, Yamamoto F, Nakano S. Pain treatment by spinal cord stimulation. *Clinical Electroencephalography (Japan)* 2005;14:7–17. (In Japanese).
6. Kumar K, Hunter G, Demeria D. Spinal cord stimulation in treatment of chronic benign pain: challenges in treatment planning and present status, a 22-year experience. *Neurosurgery* 2006;58:481–496.
7. North RB, Kidd DH, Farrokhi F, Piantadosi SA. Spinal cord stimulation versus repeated lumbosacral spine surgery for chronic pain: a randomized controlled trial. *Neurosurgery* 2005;56:98–107.
8. Kumar K, North R, Taylor R et al. Spinal cord stimulation vs. conventional medical management: a prospective, randomized, controlled, multi center study of patients with failed back surgery syndrome (PROCESS Study). *Neuromodulation* 2005;8:213–218.
9. Stanton-Hicks MD, Burton AW, Bruehl SP et al. An updated interdisciplinary clinical pathway for CRPS: report of an expert panel. *Pain Pract* 2002;2:1–16.
10. Forouzanfar T, Kemler MA, Weber WE, Kessels AG, van Kleef M. Spinal cord stimulation in complex regional pain syndrome: cervical and lumbar devices are comparably effective. *Br J Anaesth* 2004;92:348–353.
11. Reig E, Abejón D, del Pozo C, Wojcikiewicz R. Spinal cord stimulation in peripheral vascular disease: a retrospective analysis of 95 cases. *Pain Pract* 2001;1:324–331.
12. The EuroQol Group. EuroQol—a new facility for the measurement of health-related quality of life. *Health Policy* 1990;16:199–208.
13. Moriyama K. Effect of temporary spinal cord stimulation on postherpetic neuralgia in the thoracic nerve area. *Neuromodulation* 2009;12:39–43.
14. Mingyuan W, Linderoth B, Foreman RD. Putative mechanisms behind effects of spinal cord stimulation on vascular diseases: a review of experimental studies. *Autonomic Neuroscience: Basic & Clinical* 2008;138:9–23.
15. Smith BH, Macfarlane GJ, Torrance N. Epidemiology of chronic pain, from the laboratory to the bus stop: time to add understanding of biological mechanisms to the study of risk factors in population-based research? *Pain* 2007;127:5–10.
16. Pruijboom L, van Dam AC. Chronic pain: a non-use disease. *Med Hypotheses* 2007;68:506–511.
17. Livingston WK. *Pain mechanism: a physiologic interpretation of causalgia and its related states*. New York, NY: MacMillan, 1943.

COMMENTS

The findings demonstrated specifically regarding Failed Back Surgery Syndrome, are critical in further understanding the mechanisms involved in Neuromodulation. The use of a mixed model analysis brings to the forefront, the complexity of Failed Back Surgery Syndrome. The authors have done a good job of separating the peripheral and central differences in response to Neuromodulation.

Yeshvant Navalgund, M.D.
Pittsburgh, PA USA

In this multicenter study of spinal cord stimulation (SCS), 55 patients with complex regional pain syndrome (CRPS), failed back surgery syndrome (FBSS), and peripheral vascular disease (PVD) were recruited. After a test stimulation, chronic implantation was performed in 34 out of the 55 patients. Generally, all of the CRPS, FBSS, and PVD patients recruited are good candidates for SCS therapy. However, the rate of chronic implantation was 34/55 (60%) in this study. On the basis of logistic model analysis, 1) cover rate, 2) gender, and 3) the part of the nervous system affected as the authors described, were selected as the good predictors of a successful SCS therapy. I think that the pharmacological evaluation of each patient before a test stimulation is very important to increase the success rate of the test stimulation. This is called a drug challenge test and is generally applied in Japan. The drug challenge test (1), in which the drugs tested include morphine, barbiturate, and ketamine, is important for increasing the success rate of SCS and is also useful for finding the drugs that complement SCS therapy.

1. Yamamoto T, Katayama Y, Hirayama T, Tsubokawa T: Pharmacological classification of central post-stroke pain; comparison with the results of chronic motor cortex stimulation therapy. *Pain* 72: 5–12, 1997

Takamitsu Yamamoto, M.D., Ph.D.
Tokyo, Japan

Comments not included in the Early View version of this paper.

在宅型反復経頭蓋磁気刺激治療のための 磁場ナビゲーションシステムの開発

福島 大志 ・ 西川 敦 ・ 宮崎 文夫 ・ 関野 正樹
安室 喜弘 ・ 松崎 大河 ・ 細見 晃一 ・ 齋藤 洋一

生体医工学 Vol. 49 No. 1 別冊(2011)

日本生体医工学会

在宅型反復経頭蓋磁気刺激治療のための 磁場ナビゲーションシステムの開発

福島 大志*・西川 敦**,***・宮崎 文夫*・関野 正樹**,†
安室 喜弘**,††・松崎 大河**,†††・細見 晃一**・齋藤 洋一**

The Development of Magnetic Navigation System for Home Use of Repetitive Transcranial Magnetic Stimulation

Taishi FUKUSHIMA,* Atsushi NISHIKAWA,**,*** Fumio MIYAZAKI,* Masaki SEKINO**,†
Yoshihiro YASUMURO**,†† Taiga MATSUZAKI**,††† Koichi HOSOMI,** Youichi SAITOH**

Abstract Repetitive Transcranial Magnetic Stimulation (rTMS) is effective for intractable diseases of the nervous system. As the effects of rTMS last only several hours, rTMS therapies need to be continued daily. Under present circumstances, it is difficult to use rTMS in patients' home, because only experienced physicians in limited hospitals can use the expensive and complicated rTMS system. Therefore, we developed a magnetic navigation system for home use of rTMS. The proposed system uses inexpensive and small magnetic sensors; hence it is suitable for home use. By using the proposed method, even people who have no medical knowledge and technique can easily navigate the coil to the optimal position preliminarily specified by expert physicians. Our system needs to collect some dataset which consists of magnetic field and the corresponding position of the coil at the patients' initial visit. Since it is bothersome to collect a large number of dataset, we reduced the dataset by approximation using multi-regression analysis.

Keywords : rTMS, home treatment, magnetic navigation, multi-regression analysis.

1. はじめに

今日、鬱病、神経障害性疼痛、パーキンソン病などの難治性の精神および神経疾患に悩む患者は急速に増えている[1]。反復経頭蓋磁気刺激 (rTMS) がこれら疾患に対して有効であることが確認され始め、rTMS への関心は飛躍的に高まっている[2-6]。rTMS は頭皮表面に置いた刺激

コイルに電流を流しパルス磁場を生じさせ、電磁誘導を利用して刺激コイル直下の脳内神経を刺激する非侵襲的な手法である。したがって、埋め込み型電気刺激療法のような、患者によっては抵抗感の非常に大きい開頭手術が必要なく、感染症などの副作用の心配もないため、極めてメリットの多い治療法となりうる。しかし、rTMS の治療効

生体医工学シンポジウム 2010 発表 (2010 年 9 月, 札幌)
2010 年 7 月 30 日受付, 2010 年 10 月 8 日改訂, 2010 年 11 月 6 日再改訂
Received July 30, 2010; revised October 8, 2010, November 6, 2010.

* 大阪大学大学院基礎工学研究科機能創成専攻
Department of Mechanical Science and Bioengineering,
Graduate School of Engineering Science, Osaka University

** 大阪大学先端科学イノベーションセンター脳神経制御外科学

Department of Neuromodulation and Neurosurgery,
Center for Advanced Science and Innovation, Osaka
University

*** 信州大学繊維学部応用生物学系バイオエンジニアリング課程

Bioengineering Course, Division of Applied Biology,
Faculty of Textile Science and Technology, Shinshu
University

† 東京大学大学院工学系研究科電気系工学専攻
Department of Electrical Engineering and Information
Systems, Graduate School of Engineering, The University
of Tokyo

†† 関西大学環境都市工学部都市システム工学科
Faculty of Environmental and Urban Engineering, Kansai
University

††† 帝人ファーマ株式会社在宅医療開発推進部
Home Healthcare Research & Development Department,
Teijin Pharma Limited

果には持続性がない為、患者は設備の整った病院に定期的に通院しなければならない、在宅利用を行いたいという強いニーズが医師・患者双方から生じている。しかしながら、現状のシステムは非常に高価で大型な機器を用いており、そのうえ、診察の度に熟練した医師が最適刺激位置を特定しなければならない、そのまま在宅化するのは困難である。

本研究では、患者やその家族、介護者のような非医療従事者であっても、在宅において容易に患者の最適位置を特定し rTMS 治療を受けられるように、安価で小型な磁気センサを用いた rTMS コイルナビゲーションシステムを開発することを目的とする。我々は磁場逆解析ナビゲーション、データセット型磁場ナビゲーション（後述）を既に提案している [7-10]。本研究では、後者のナビゲーションに近似手法を取り入れた場合の結果について示す。また、新しいキャリブレーション手法を提案しその評価を行う。そして、実際の人間に対しナビゲーションタスクを行う実験の結果について述べることで、本ナビゲーションシステムが在宅利用可能であることを示す。

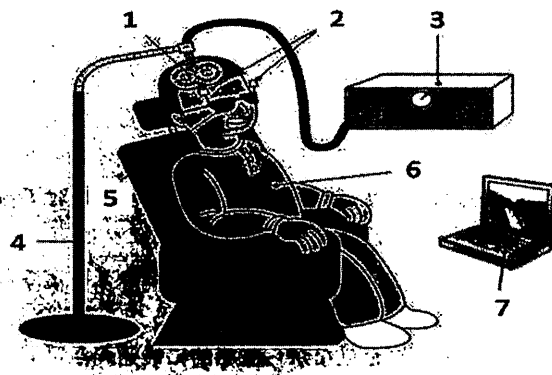
2. 方 法

2.1 システム構成

在宅におけるシステムの外観を図 1 に示す。患者は安楽椅子に座り、磁気センサを取り付けたメガネを装着する。磁気センサの計測値は A/D ボードを通して PC に送られる。刺激コイルには永久磁石が取り付けられている。刺激コイルスタンドを使うことで刺激中に刺激コイルを支えておくという負担を減らすことができる。また、患者が人の手を借りずに自身で刺激することも可能である。なお、病院においては従来の rTMS と同様に光学式トラッキングシステム (NDI 社製 POLARIS [11]) を使用する。プログラム言語は C, C++ 言語を使用し、ナビゲーション用インタフェースには OpenGL を使用した。

2.2 ナビゲーション手法

データセット型磁場ナビゲーションについて説明する。データセット [9] とは、刺激コイルに取り付けた永久磁石 (図 2) が発する磁場と刺激コイルの 3 次元位置の組み合わせ (表 1) であり、それぞれ複数の磁気センサと POLARIS を用いて同時計測する。本手法では、まず病院において患者に磁気センサの付いた固定具 (本研究では防塵メガネを利用した) を装着してもらう。次に、メガネを毎回同じ位置に装着するために永久磁石を用いてキャリブレーションを行う (2.4)。以上の準備のもとで、従来の手法 (MR 画像と光学式トラッキング座標系を合成し最適刺激位置を特定する手法 [2, 6]) により医師が最適刺激位置を特定し、最適刺激位置とその周辺のデータセットを収集する。最適刺激位置以外のデータセットは、患者の頭皮に沿うように、最適刺激位置を中心とした半径約 5 [cm] の範囲内で、最適刺激位置近傍がより密になるように刺激



1. 永久磁石付刺激コイル (磁石: ネオジム角型 20×10×10, 表面磁束密度 490[mT])
2. 磁気センサ (愛知製鋼社製 3 軸センサ AMI302 [12])
3. 磁気刺激装置本体
4. 刺激コイルスタンド
5. 磁気センサ固定具 (メガネなど)
6. 患者
7. PC (Intel Core2Duo 2.80 [GHz], メモリ 4 [GB])

図 1 提案手法在宅利用時の外観

Fig. 1 Overview of the proposed system for home use.

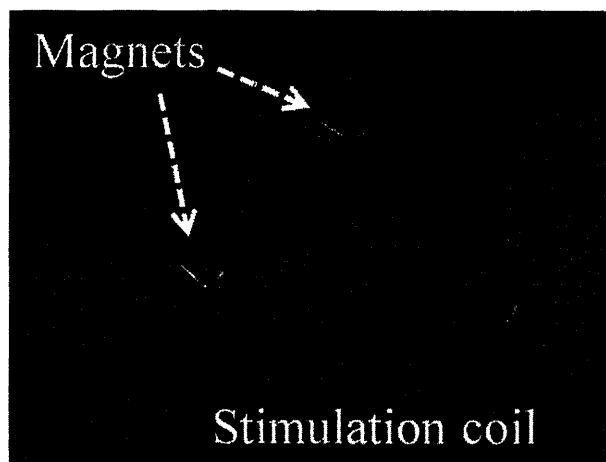


図 2 永久磁石を取り付けた刺激コイル

Fig. 2 Stimulation coil with permanent magnets mounted on.

表 1 データセット

Table 1 Dataset.

Data number	Magnetic field	Coil position
1	B_1	(P_1, R_1)
2	B_2	(P_2, R_2)
...
n	B_n	(P_n, R_n)

B : 磁気センサの計測値 (m次元ベクトル. たとえば, 3軸磁気センサを4個使用した場合 $m=12$)
 P : コイル中心の位置 R : コイルの姿勢

コイルをランダムに動かしながら収集する。最適刺激位置以外のデータセットがあることで、刺激コイルが現在どの位置にあってどの程度ずれを生じているのか、どの方向に

刺激コイルを移動させたら良いのか、視覚的に認識することが可能となる。在宅治療時はまず、病院と同じように患者はメガネを装着しキャリブレーションを行う。刺激コイルを頭部に当てると、その位置での永久磁石の発する磁場をデータセットと比較することで、刺激コイルの3次元位置が求められる(2・3)。コイルの3次元位置はOpenGL [13, 14]を利用して作成したグラフィックに表示される(図3)。さらに、モニタ上には病院において特定された最適刺激位置と刺激コイルを移動させるべき方向が表示され、患者はモニタを見ながら直感的に最適刺激位置へ刺激コイルを移動させることができる。なお、現段階では永久磁石は誘導時のみ用い、刺激時は取り外すことを想定している。これは取り外さなかった場合、刺激時に永久磁石がどのような影響を受けるのかがまだわからないためである。本実験においては刺激を行う訳ではないため、実験の簡便さから永久磁石は図2の位置に取り付けているが、取り付け位置に関してはより安全性の高い位置を今後検討していくつもりである。

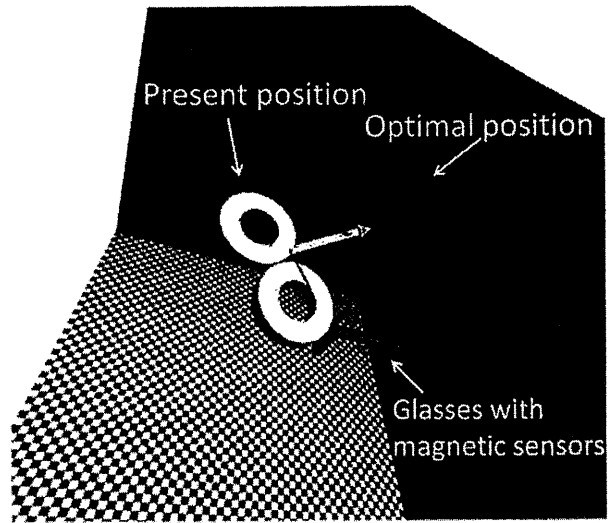


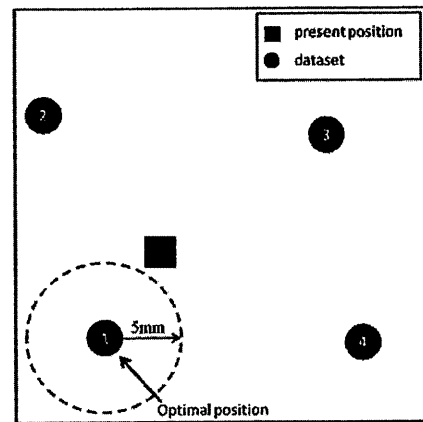
図3 OpenGL モニタ
Fig. 3 OpenGL monitor

2・3 刺激コイル位置・姿勢近似手法

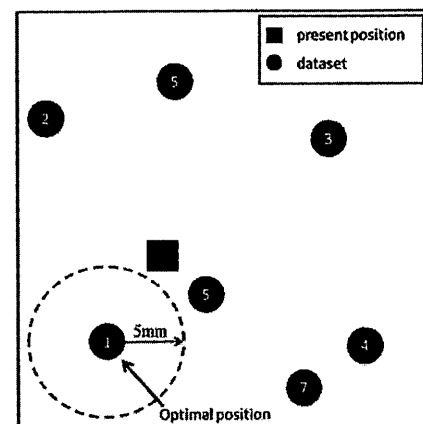
図4(a), (b)はそれぞれデータセットが少ない場合(4セット)と多い場合(7セット)を簡易的に示している。OpenGLによって表示される刺激コイルの位置は、現在の刺激コイルの位置から最も近いデータセットの位置(正確には式(1)の*f*値が最も小さいデータセットの位置であり、必ずしも最も近い訳ではないが、便宜上ここでは最も近いデータセットの位置とする)が表示される。図4(a)の場合、現在の刺激コイル位置が最適刺激位置から5[mm]以上離れているにも関わらず、最も近いデータセットである最適刺激位置の座標(1番)がモニタに表示されてしまい、刺激コイルの操作者が最適刺激位置に到達したと誤解してしまう。しかし、図4(b)の場合、現在の刺激コイルの位置に最も近いデータセットは5番のデータセットの位置であるため、その位置がモニタに表示され操作者が誤解をすることはなくなる。そのため、データセットの数が多ければ多いほど誘導精度を上げることができる。しかし、たくさんのデータを収集するのは医師の負担になってしまう。そこで、データセットの数を減らすためにデータセットの近似を行う。我々は近似手法として重回帰分析を応用する[15]。まず、磁気センサがリアルタイムに取得したデータを*A*とする(患者が刺激コイルを置いた位置での磁場)。*A*と*n*個のデータセットの磁場を比較し、式(1)の*f*値をそれぞれのデータセットで求める。

$$f_i = \frac{1}{2} \sum_{\alpha=1}^{12} |A_{\alpha} - B_{i\alpha}|^2 \quad (1)$$

式(1)では比較するデータセットナンバーを添字*i*で表す(*f*₁~*f*_{*n*})。また、どの磁気センサが取得した計測値かを添字*α*で表す(本研究では3軸磁気センサを4個使用しているため式(1)中の*α*は1~12である)。次に、データ



(a) データセットが少ない場合 (4セット)
(a) The case that there are a few dataset (4 sets)



(b) データセットが多い場合 (7セット)
(b) The case that there are many dataset (7 sets)

図4 データセット数の影響

Fig. 4 The influence of the number of dataset.

セットの中から f 値の小さいものを 10 組抽出する。その 10 組の磁場データを並べた 12 行 10 列の磁場の組み合わせを行列 C とする。一般に、重回帰分析は被説明変数を Y , 説明変数を x_1, \dots, x_k , 回帰係数を $\theta_0, \theta_1, \dots, \theta_k$, 誤差を ε とした式(2)で表される関係式を利用する。本研究の場合、12 個のセンサ計測値それぞれに式(2)のような関係式が作られる (被説明変数: センサ計測値, 説明変数: 抽出した 10 組のデータセット)。12 個の関係式をまとめてベクトル表記すると式(3)のように表せる。

$$Y = \theta_0 + \theta_1 x_1 + \dots + \theta_k x_k + \varepsilon \quad (2)$$

$$A = \mathbf{1}\theta_0 + C\theta + \varepsilon \quad (3)$$

ここで、 $A = (A_1, \dots, A_{12})^T$, $\mathbf{1} = (1, \dots, 1)^T$, ε は 12 次元列ベクトル, θ_0 , θ は回帰係数であり θ は 10 次元列ベクトルである。次に式(3)から θ の最小二乗推定量 $\hat{\theta}$ を求める。この $\hat{\theta}$ を用いて、磁気センサの値が A の時の刺激コイルの位置 P_A ・姿勢 R_A を次の式(4), 式(5)のように近似する。なお、選択した 10 個のデータセットを添字 i で区別している。

$$P_A = \frac{\sum_{i=1}^{10} |\hat{\theta}_i| P_i}{\sum_{i=1}^{10} |\hat{\theta}_i|} \quad (4)$$

$$R_A = \frac{\sum_{i=1}^{10} |\hat{\theta}_i| R_i}{\sum_{i=1}^{10} |\hat{\theta}_i|} \quad (5)$$

これにより求めた P_A , R_A が図 3 のモニタにリアルタイムに表示される。

なお、近似手法を用いない場合には、式(1)の f 値が最も小さいデータセットに対応する刺激コイル位置・姿勢をそのまま P_A , R_A として出力する。

2.4 キャリブレーション手法

我々の提案手法において、磁気センサを固定しているメガネは、病院で装着した際と同じ位置に在宅においても装着されることが前提である。本研究で我々の使用したメガネは防塵メガネであり、もともとずれにくい設計にはなっているものの、やはり個人差があり何らかのキャリブレーションが必要である。本研究ではメガネに装着している磁気センサをそのまま利用してキャリブレーションを行う。

図 5 のようにメガネの中央にゴム板を取付け、先端に永久磁石を脱着できるようにする。このゴム板は患者の鼻の形状に沿って曲がるようになっている。キャリブレーションの手順は次の通りである。まず、病院において患者は適当な位置にメガネを装着する。その時、ゴム先端に永久磁石を付けた状態と付けてない状態の磁場の差を記録する (この差を 12 次元ベクトル D とする)。在宅においても同様に、永久磁石を付けていない状態と付けた状態での磁場の差を記録する (この差を 12 次元ベクトル E とする)。 D , E のように磁場の差を記録するのは地磁気や環

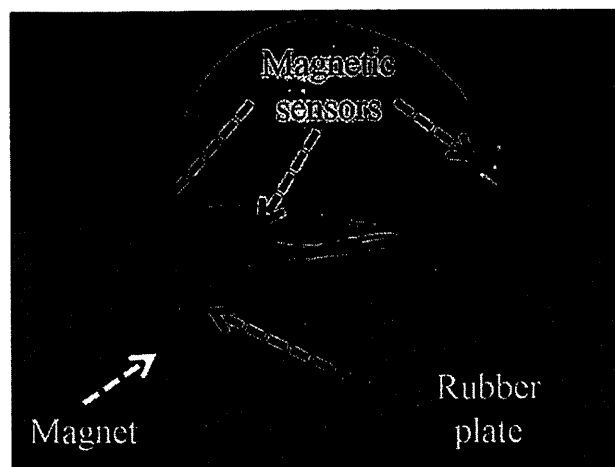


図 5 磁気センサ固定メガネ

Fig. 5 The glasses with magnetic sensors mounted on.

表 2 g_{th} と誤差の相関

Table 2 The correlation between g_{th} and the error of distance.

g_{th}	the error of distance[mm]		
	1st trial	2nd trial	3rd trial
0.0005	7.93	5.84	5.99
0.0001	2.73	1.42	2.54
0.00005	1.67	2.44	2.43

境磁場の影響を排除する為である。もし差ではなく永久磁石を付けた状態の磁場のみを記録した場合、その記録した磁場には地磁気や環境磁場による磁場が含まれる。地磁気や環境磁場は病院や患者の自宅において異なるので、差を利用することで永久磁石による磁場のみを計測でき他の影響を排除することができる。次にこれら D , E を式(6)に代入し、 g 値を計算する。この g 値が最小となるように患者がメガネの位置を調整することでキャリブレーションを行うことができる。

$$g = \frac{1}{2} \sum_{\alpha=1}^{12} |D_{\alpha} - E_{\alpha}|^2 \quad (6)$$

ここで式(1)と同様に、どの磁気センサが取得した計測値かを添字 α で表す。

3. 実 験

3.1 キャリブレーション

2.4 のキャリブレーションを評価する為の実験を行った。初めに被験者に最適位置にメガネを装着してもらい D を記録し、POLARIS を用いてメガネの位置を記録しておく。その後、メガネを一旦外し再度装着した際に E を計測する。これらから式(6)の g を算出し、 g がある閾値 g_{th} 以下になった際にピープ音を鳴らす。被験者はピープ音が鳴るようにメガネを調整し、調整終了後のメガネの位

置を POLARIS を用いて計測し最適位置との誤差を評価する。まず、 g_{th} を定めるために患者頭部を模擬したモデルを利用しメガネの脱着を繰り返し行い、 g_{th} と誤差の相関を実験的に算出した (表 2)。rTMS において最適刺激位置は直径 10[mm] 程度である [16] ので、メガネの誤差も半径 5[mm] 以内となるように $g_{th} = 0.0001$ と設定した。被験者数は非医療従事者 20 代男性 3 名 (被験者 A, B, C とする) であり、それぞれ 3 回ずつメガネを脱着するというタスクを行ってもらい誤差を計測した。

3.2 ナビゲーションタスク 1

近似手法の有効性を検証するために、まず、近似手法を用いずに最適刺激位置へ刺激コイルを誘導できるかどうか実験を行った。本実験では在宅における刺激コイル操作者は、患者ではなくホームヘルパーや患者の家族などという設定にした。また、このタスクではメガネのキャリブレーションの誤差の影響を排除するため、患者の代わりに患者頭部を模擬したモデルを使用し磁気センサを直接模型に固定した。被験者には OpenGL モニタを見ながら頭部模型上で刺激コイルを操作してもらい、最適刺激位置の指定及びデータセットの収集は筆者が行った。被験者は非医療従事者 20 代男性 3 名であり 3.1 と同じ人物である。測定した内容は最適刺激位置との誤差と最適刺激位置までの誘導にかかる時間である。最適刺激位置との誤差は POLARIS を用いて測定した。また、データセット数が 500 個の場合と 1000 個の場合の 2 つのパターンで実験を行った。データセットは最適刺激位置付近を中心に集めている。被験者には各場合 3 回ずつ計 6 回、刺激コイルを最適刺激位置まで誘導させるというタスクを行ってもらった。被験者にはナビゲーションを始める前に操作に慣れるために 3 分間の練習を行ってもらい実験を開始した。

3.3 ナビゲーションタスク 2

2.3 の近似手法を用いて 3.2 と同様の実験を行った。本実験ではデータセットの数は 500 個の場合のみである。被験者は非医療従事者 20 代男性 3 名であり 3.1, 3.2 と同じ人物である。

3.4 ナビゲーションタスク 3

3.2, 3.3 では頭部模型を患者に見立てて実験を行った。本実験では実際に被験者 D に患者役としてメガネをかけてキャリブレーションを行ってもらい、被験者 E にナビゲーションタスクを行ってもらった。被験者 D, E は共に非医療従事者 20 代男性であり被験者 A, B, C とは異なる者である。近似手法を用い、データセットは 500 個収集した。ナビゲーションタスクは計 3 回行った。

3.5 インフォームドコンセント

本研究における全ての被験者には事前に本実験の目的と本実験が実際に刺激を行う訳ではなく安全であることを十分に説明し、理解してもらった上で本実験への協力の同意を得ている。

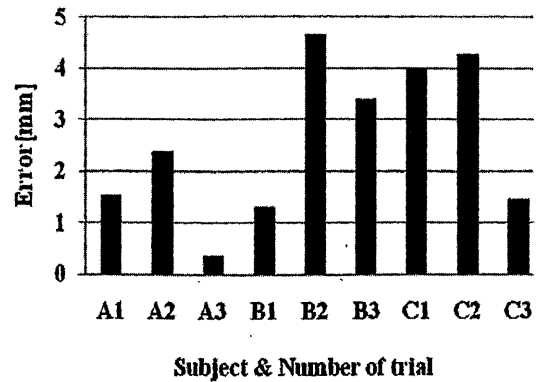


図 6 距離誤差

Fig. 6 Error of length

4. 結果・考察

4.1 キャリブレーション

図 6 は被験者 A, B, C にそれぞれ 3 回ずつメガネの脱着を繰り返してもらった際の最適位置との誤差を示している。結果をみると、全試行において 5[mm] 以内の誤差に収まっていることがわかる。キャリブレーションにかかる時間は全試行において 30[s] 以内であった。このキャリブレーション手法はカメラなど高価な機器を必要としないことから在宅化する際にコスト面でメリットは大きい。しかしながら、rTMS を用いた治療は刺激部位に対して mm 単位の精度が必要であり、精度が上がるほど良い治療効果が見込まれることから更なる改善が必要である。改善案としてはメガネバンドを利用することや、水泳用のゴーグルのようにより頭部にフィットするものを利用することなどが考えられ、これらについては今後検討する予定である。装着具はものによっては患者の不快感等、主観的評価がなされるため選定基準は難しいが、今後位置決め精度を上げていくために他種のメガネや、その他代替手段についても検討し、より位置決め精度の高い装着具を選定する必要がある。

4.2 ナビゲーションタスク 1

図 7~図 11 は被験者 A, B, C にそれぞれデータセットが 500 個の場合と 1000 個の場合について 3 回ずつ一人計 6 回ナビゲーションタスクを行ってもらった時の最適位置との距離誤差、各軸回りの誤差、試行時間を示している。図 12 は図 7~図 11 の平均値と標準偏差を示している (例えば length 項の系列 500 の場合、図 7 の系列 500 の 9 回のタスクの平均値と標準偏差)。結果から、データセット数が多くなると誤差が大きくなり減少していることがわかる。500 個の場合はやや誤差が大きいが、1000 個の場合だと治療効果が最も有効に得られるとされる 5[mm], 5 [deg] 以内の誤差にはほぼ収まっており十分利用可能であると考えられる [16]。表 3 はデータセットが 500 個と 1000

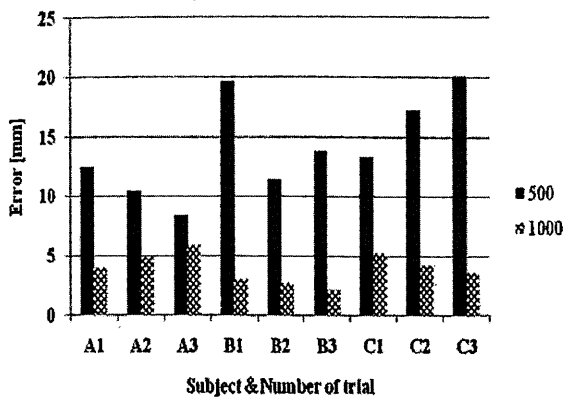


図 7 距離誤差
Fig. 7 Error of length

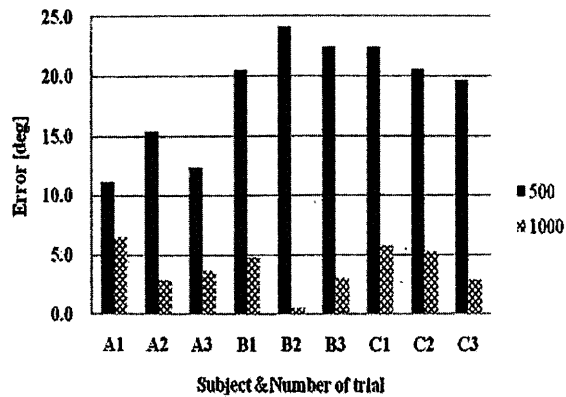


図 10 ヨー角誤差
Fig. 10 Error of yaw angle

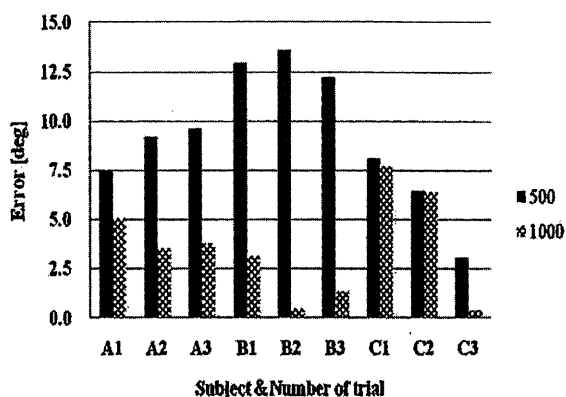


図 8 ロール角誤差
Fig. 8 Error of roll angle

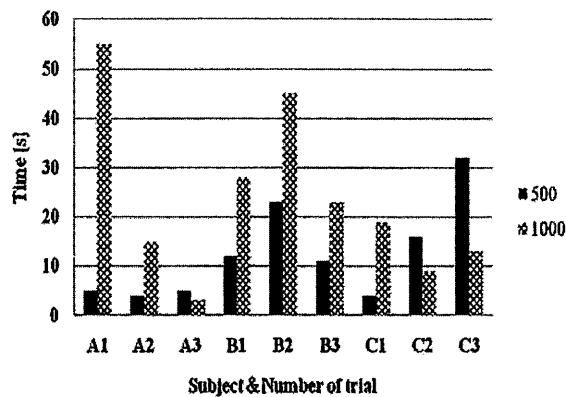


図 11 試行時間
Fig. 11 Trial time

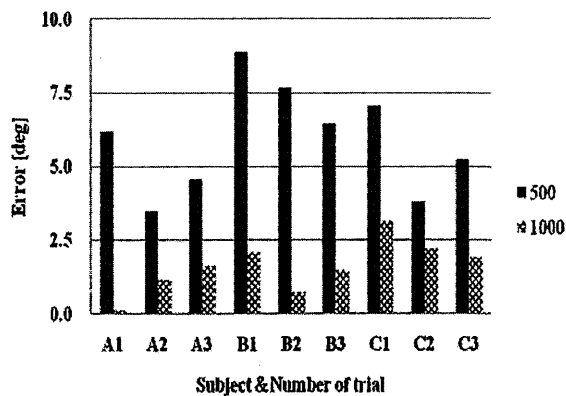


図 9 ピッチ角誤差
Fig. 9 Error of pitch angle

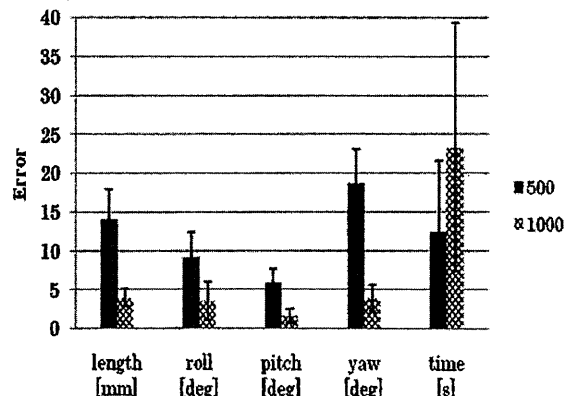


図 12 平均値と標準偏差
Fig. 12 Average and standard deviation

表 3 t 検定における P 値
Table 3 P value in the t-test

	length	roll	pitch	yaw	time
P	5.69E-05	1.05E-03	8.27E-06	4.72E-06	0.114

置を POLARIS を用いて計測し最適位置との誤差を評価する。まず、 g_{th} を定めるために患者頭部を模擬したモデルを利用しメガネの脱着を繰り返し行い、 g_{th} と誤差の相関を実験的に算出した (表 2)。rTMS において最適刺激位置は直径 10[mm] 程度である [16] ので、メガネの誤差も半径 5[mm] 以内となるように $g_{th} = 0.0001$ と設定した。被験者数は非医療従事者 20 代男性 3 名 (被験者 A, B, C とする) であり、それぞれ 3 回ずつメガネを脱着するというタスクを行ってもらい誤差を計測した。

3.2 ナビゲーションタスク 1

近似手法の有効性を検証するために、まず、近似手法を用いずに最適刺激位置へ刺激コイルを誘導できるかどうか実験を行った。本実験では在宅における刺激コイル操作者は、患者ではなくホームヘルパーや患者の家族などという設定にした。また、このタスクではメガネのキャリブレーションの誤差の影響を排除するため、患者の代わりに患者頭部を模擬したモデルを使用し磁気センサを直接模型に固定した。被験者には OpenGL モニタを見ながら頭部模型上で刺激コイルを操作してもらう。最適刺激位置の指定及びデータセットの収集は筆者が行った。被験者は非医療従事者 20 代男性 3 名であり 3.1 と同じ人物である。測定した内容は最適刺激位置との誤差と最適刺激位置までの誘導にかかる時間である。最適刺激位置との誤差は POLARIS を用いて測定した。また、データセット数が 500 個の場合と 1000 個の場合の 2 つのパターンで実験を行った。データセットは最適刺激位置付近を中心に集めている。被験者には各場合 3 回ずつ計 6 回、刺激コイルを最適刺激位置まで誘導させるというタスクを行ってもらった。被験者にはナビゲーションを始める前に操作に慣れるために 3 分間の練習を行ってもらい実験を開始した。

3.3 ナビゲーションタスク 2

2.3 の近似手法を用いて 3.2 と同様の実験を行った。本実験ではデータセットの数は 500 個の場合のみである。被験者は非医療従事者 20 代男性 3 名であり 3.1, 3.2 と同じ人物である。

3.4 ナビゲーションタスク 3

3.2, 3.3 では頭部模型を患者に見立てて実験を行った。本実験では実際に被験者 D に患者役としてメガネをかけてキャリブレーションを行ってもらい、被験者 E にナビゲーションタスクを行ってもらった。被験者 D, E は共に非医療従事者 20 代男性であり被験者 A, B, C とは異なる者である。近似手法を用い、データセットは 500 個収集した。ナビゲーションタスクは計 3 回行った。

3.5 インフォームドコンセント

本研究における全ての被験者には事前に本実験の目的と本実験が実際に刺激を行う訳ではなく安全であることを十分に説明し、理解してもらった上で本実験への協力の同意を得ている。

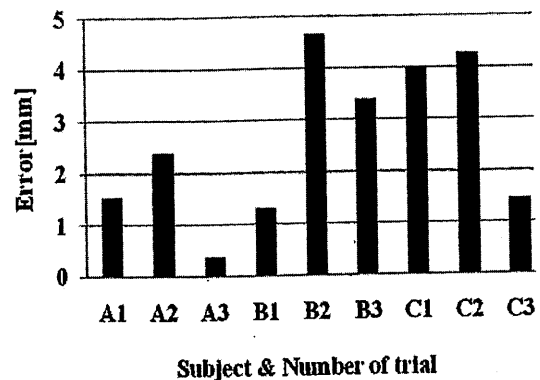


図 6 距離誤差

Fig. 6 Error of length

4. 結果・考察

4.1 キャリブレーション

図 6 は被験者 A, B, C にそれぞれ 3 回ずつメガネの脱着を繰り返してもらった際の最適位置との誤差を示している。結果をみると、全試行において 5[mm] 以内の誤差に収まっていることがわかる。キャリブレーションにかかる時間は全試行において 30[s] 以内であった。このキャリブレーション手法はカメラなど高価な機器を必要としないことから在宅化する際にコスト面でメリットは大きい。しかしながら、rTMS を用いた治療は刺激部位に対して mm 単位の精度が必要であり、精度が上がるほど良い治療効果が見込まれることから更なる改善が必要である。改善案としてはメガネバンドを利用することや、水泳用のゴーグルのようにより頭部にフィットするものを利用することなどが考えられ、これらについては今後検討する予定である。装着具はものによっては患者の不快感等、主観的評価がなされるため選定基準は難しいが、今後位置決め精度を上げていくために他種のメガネや、その他代替手段についても検討し、より位置決め精度の高い装着具を選定する必要がある。

4.2 ナビゲーションタスク 1

図 7~図 11 は被験者 A, B, C にそれぞれデータセットが 500 個の場合と 1000 個の場合について 3 回ずつ一人計 6 回ナビゲーションタスクを行ってもらった時の最適位置との距離誤差、各軸回りの誤差、試行時間を示している。図 12 は図 7~図 11 の平均値と標準偏差を示している (例えば length 項の系列 500 の場合、図 7 の系列 500 の 9 回のタスクの平均値と標準偏差)。結果から、データセット数が多くなると誤差が大きくなり減少していることがわかる。500 個の場合はやや誤差が大きいが、1000 個の場合だと治療効果が最も有効に得られるとされる 5[mm], 5 [deg] 以内の誤差にほぼ収まっており十分利用可能であると考えられる [16]。表 3 はデータセットが 500 個と 1000